Modelling Nifedipine Photodegradation, Photostability and Actinometric Properties.

Wassila MAAFI • Mounir MAAFI*

Leicester School of Pharmacy, De Montfort University, The Gateway, Leicester, LE1 9BH, UK.

Corresponding author: (Mounir Maafi)

Email: mmaafi@dmu.ac.uk

Tel: +44 116 257 7704.

Fax: +44 116 257 7287.

ABSTRACT

Background

The photodegradation of drugs obeying unimolecular mechanisms such as that of Nifedipine (NIF) were usually characterized in the literature by zero-, first- and second-order kinetics. This approach has been met with varying success. This paper addresses this issue and proposes a novel approach for unimolecular photodegradation kinetics. The photodegradation of the cardiovascular drug Nifedipine is investigated within this framework.

Methods

Experimental kinetic data of Nifedipine photodegradation were obtained by continuous monochromatic irradiation and DAD analysis. Fourth-order Runge-Kutta calculated kinetic data served for the validation of the new semi-empirical integrated rate-law model proposed in this study.

Results

A new model equation has been developed and proposed which faithfully describes the kinetic behaviour of NIF in solution for non-isosbestic irradiations at wavelengths where both NIF and its photoproduct absorb. NIF absolute quantum yield values were determined and found to increase with irradiation wavelength according to a defined sigmoid relationship. The effects of increasing NIF or excipients' concentrations on NIF kinetics were successfully modelled and found to improve NIF photostability. The potential of NIF for actinometry has been explored and evaluated. A new reaction order (the so-called *Φ-order*) has been identified and specifically proposed for unimolecular photodegradation reactions.

Conclusion

The semi-empirical and integrated rate-law models facilitated reliable kinetic studies of NIF photodegradation as an example of AB(1Φ) unimolecular reactions. It allowed filling a gap in kinetic studies of drugs since, thus far, thermal first-order or a combination of first- and zero-order kinetic equations were generally applied for drug photoreactions in the literature. Also, a new reaction order, the "Φ-order", has been evidenced and proposed as a specific alternative for photodegradation kinetics.

KEY WORDS Nifedipine • photodegradation • modelling • photostability • actinometry.

1. INTRODUCTION

Nifedipine (NIF) is a dihydropyridine derivative that belongs to the calcium-channel blockers family (Piechocki and Thoma, 2010; Tonnesen, 2004; Albini and Fasani, 1998). It is used for mild to moderate hypertension (Kawabe et al., 2008). NIF is one of the most known photolabile drugs (Piechocki and Thoma, 2010; Tonnesen, 2004; Albini and Fasani, 1998) yielding a pharmacologically inert photoproduct. However, it is not totally clear whether the photodecomposition process leads to toxic species (Onoue et al., 2008; Pizzaro-Urzua and Nunez-Vergara, 2005; De Vries and Henegouwen, 1998).

A number of kinetic methods have been proposed to study the photodecomposition of NIF (Piechocki and Thoma, 2010; Tonnesen, 2004; Albini and Fasani, 1998; Pietta et al., 1981; Fasani et al., 2006; Gorner, 2010). Separation techniques were largely preferred because they allow monitoring the kinetic evolution of NIF concentration throughout the photodegradtion reaction. Conversely, the spectroscopic methods, including spectrophotometry, were rarely employed for such studies mainly because of the overlapping of the spectra of NIF and its photoproduct.

The treatment of such kinetic data was generally achieved by using the equations developed for the zero- and/or first-order thermal reactions (Sangoi et al., 2013; Mattos et al., 2012; Piechocki and Thoma, 2010; Souza et al., 2010; Shamsipur et al., 2003; Thoma and Klimek, 1991, Albini and Fasani, 1998; Majeed and Murray, 1987). A fewer number of studies proposed approaches to rationalise the photodegradation kinetics with other models (Matsuda

et al., 1995; Mielcarek et al., 2005) than the zero and first-order integrated rate laws. In this respect, modelling photoreaction has been a critical issue due the difficulty in solving the differential equation of photoreactions (Mauser and Gauglitz, 1998; Maafi and Brown, 2005; Maafi and Brown, 2007; Maafi and Brown, 2008; Maafi, 2010; Maafi, 2008). Mathematical complications arise from the presence of the time-dependent photokinetic factor that renders integration difficult if at all possible.

Building on our studies relative to modelling the kinetics of unimolecular photochemical reactions (Maafi and Brown, 2005; Maafi and Brown, 2007; Maafi and Brown, 2008; Maafi, 2010; Maafi, 2008), we propose, in this study, to develop a strategy for describing the kinetics of NIF for a set of situations involving a range of irradiation and experimental conditions. The usefulness of this strategy is finally tested for NIF-actinometery.

2. MATERIALS AND METHODS

2.1. Materials

Nifedipine, 3,5-dimethyl 2,6-dimethyl-4-(2-nitrophenyl)-1,4-dihydropyridine-3,5-dicarboxylate, (NIF), tartrazine, (TRZ), sunset yellow, (SSY), quinoline yellow, (QY), and spectrophotometric grade ethanol were purchased from Aldrich and were used without further purification.

2.2. Monochromatic continuous irradiation/monitoring set up

The absorption spectra and kinetic profiles were recorded on an Agilent 8453 diode array spectrophotometer. The sample holder (designed for a 1-cm cell, i.e., $l_{obs} = 1$ cm) was equipped with a temperature control Peltier system model Agilent 8453. The irradiation equipment was manufactured by Photon Technology International Corporation. The light source was an Ushio 1000 W xenon arc-lamp located in a housing shell model A6000 and powered by a model LPS-1200 power supply. The lamp housing was connected to a model 101 monochromator, which is a special f/2.5 monochromator with a 1200 groove/300 nm blaze grating to allow irradiation wavelength selection. The excitation beam was guided through an optical fibre to impinge upon the top of the sample cuvette. Hence, the directions of irradiation and analysis light beams were perpendicular and these lights may travel different optical path lengths inside the sample ($l_{obs} \neq l_{irr}$) .

The sample was maintained at 22°C and was stirred continuously during the experiment. In the instrumental set up used here, the sample was almost completely shielded from ambient light and the studied solution can be irradiated (λ_{irr}) and monitored (λ_{obs}) at different wavelengths ($\lambda_{irr} \neq \lambda_{obs}$).

NIF photoreaction was studied in ethanol by subjecting the solution to a continuous irradiation at a given monochromatic light beam.

The radiant power was measured on Radiant Power/Energy meter model 70260.

The values obtained from the radiant meter (in W) were divided by the product of the energy associated with a mole of photons for the selected irradiation wavelength, $E_{\lambda_{irr}} = Nhc / \lambda_{irr}$ (expressed in J mol^{-1} or J $einstein^{-1}$, with *N* the Avogadro number, *h*, Planck constant and *c*, the velocity of light), and the volume of the solution irradiated (in dm^3). Hence, the radiant power used for this study is expressed in einstein s^{-1} dm^{-3}. This unit of the radiant power is preferred as it is relevant to the kinetic study and the determination of the reaction attributed from the reaction rate-constant (k) equations (*vide infra* Eqs. 4, 6 and 8).

2.3. Treatment of the data

A Levenberg-Marquardt iterative programme within the Origin 6.0 software package was used to run the non-linear fitting and the determination of the best fit curves.

The theoretical numerical integration has been constructed on the basis of the fourth-order Runge-Kutta method (results obtained from a homemade programme).

The experimental measurements, realised in triplicates, have less than 10% standard deviation.

2.4. NIF solutions and irradiation of the reactive medium

A stock solution of NIF 8.6 x 10^{-4} M in ethanol, maintained at low temperatures in the dark, was used to prepare fresh analytical solutions of lower concentrations for irradiation. All solutions were shielded from light by aluminium foil protection.

Such fresh solutions of NIF were each submitted to an irradiation at a different wavelength. A set of wavelengths, spanning the whole absorption spectrum of NIF (λ_{irr} = 223, 235, 250, 282, 321, 345, 370 and 390 nm), were selected to study the variation of the reaction quantum yield with irradiation.

Ethanolic solutions of NIF concentrations ranging between 2.5 x 10^{-6} and 1.5 x 10^{-4}, spanning the linearity range of NIF (A_{NIF}^{390} = 2677 x C + 0.0046, r^2 = 0.999), were irradiated in very similar experimental conditions at isosbestic and non-isosbestic wavelengths 390, 354, 321 and 281 nm, where either only NIF or both NIF and PP absorb.

Four wavelengths (λ_{irr} = 321, 345, 370 and 390 nm), spanning the whole UVA-visible spectrum of NIF, were selected for the actinometric study. Each of these wavelengths was used for the irradiation of a NIF ethanolic solution for a series of "*j*" experiments that were carried out with *j* radiant power values ranging between 5 x 10^{-8} and 9 x 10^{-7} einstein s^{-1} dm^{-3}.

In order to quantify the effect of excipients on improving the photostability of NIF, we have selected three excipent-dyes, namely, Tartrazine (TRZ), Sunset Yellow (SSY), and Quinoline Yellow (QY). For this study of the effects of dyes' concentrations, a given solution of a dye was used as a background to blank the spectrophotometer (the blank experiment), then an amount of NIF (in µL) was added to the solution. This allows the exclusive observation of the variation of NIF spectra (i.e. the spectra of dye and solvent are not observed). In this study, the amount of the dye used to reduce NIF photoactivity in solution was kept within the limits of the linearity range of each dye individual calibration graph (at 390 nm, TRZ: $A_{TRZ} = 16211 \times$

$C_{TRZ} - 0.066$ ($r^2 = 0.999$) , SSY: $A_{SSY} = 13797 \times C_{SSY} + 0.0027$ ($r^2 = 0.999$) , QY: $A_{QY} = 18568 \times C_{QY} - 0.0085$ ($r^2 = 0.999$)).

3. RESULTS

3.1. The integrated rate-law models

The differential equation expressing the time variation of NIF and photoproduct (PP) concentrations (C_{NIF}(t) and C_{PP}(t), respectively, Scheme 1) is given by Eq.1. This is established considering that the solution, subjected to a monochromatic and continuous irradiation, is homogeneously and continuously stirred. It is also assumed that the concentration of the excited-state species and intermediates is negligible, the medium temperature is constant, and at the irradiation wavelength (λ_{irr}) species NIF and PP may absorb different amounts of light ($P_{\lambda_{irr}}$), i.e. the absorption coefficients (ε) of the species may be different ($\varepsilon_{NIF}^{\lambda_{irr}} \neq \varepsilon_{PP}^{\lambda_{irr}} \neq 0$) (Maafi and Brown, 2005; Maafi and Brown, 2007).

$$\frac{dC_{NIF}(t)}{dt} = -\frac{dC_{PP}(t)}{dt} = -\Phi_{NIF\rightarrow PP}^{\lambda_{irr}} \times \varepsilon_{NIF}^{\lambda_{irr}} \times l_{\lambda_{irr}} \times P_{\lambda_{irr}} \times F_{\lambda_{irr}} \times C_{NIF}(t) \qquad (Eq.1)$$

where $\Phi_{NIF\rightarrow PP}^{\lambda_{irr}}$ is the forward quantum yield of NIF phototransformation realised at the irradiation wavelength (λ_{irr}), $P_{\lambda_{irr}}$ is the radiant power, $l_{\lambda_{irr}}$ is the optical path length of the irradiation beam inside the sample, and $F_{\lambda_{irr}}$ the photokinetic factor expressed as

$$F_{\lambda_{irr}} = \frac{1 - 10^{-\left(A_{tot}^{\lambda_{irr}/\lambda_{irr}}(t) \times \frac{l_{\lambda_{irr}}}{l_{\lambda_{obs}}}\right)}}{A_{tot}^{\lambda_{irr}/\lambda_{irr}}(t) \times \frac{l_{\lambda_{irr}}}{l_{\lambda_{obs}}}} \qquad (Eq.2)$$

where $l_{\lambda_{obs}}$ is the optical path length of the monitoring light inside the sample (that may or may not be equal to $l_{\lambda_{irr}}$), $A_{tot}^{\lambda_{irr}/\lambda_{irr}}(t)$ is the total absorbance of the reaction medium (i.e. the sum of the absorbances at λ_{irr}, of all the species present in solution). Absorbances and traces are labelled here as, $\lambda_{irr}/\lambda_{obs}$, which are respectively the specific irradiation and observation wavelengths used for the experiment. Therefore, when the solution is irradiated and observed at the same (irradiation) wavelength its absorbance is labelled, $\lambda_{irr}/\lambda_{irr}$ (Eq.2). It is worth noting that, in the present paper the observed absorbances reported in the equations correspond to those measured by the monitoring beam, i.e. along $l_{\lambda_{obs}}$ where for example, $A_{tot}^{\lambda_{irr}/\lambda_{obs}}(t) = \left(C_{NIF}(t) \times \varepsilon_{NIF}^{\lambda_{obs}} + C_{PP}(t) \times \varepsilon_{PP}^{\lambda_{obs}}\right) \times l_{\lambda_{obs}}$. The absorbances corresponding to the reaction medium absorption of the irradiation light, which may not directly be accessible by the spectrophotometric measurements, when $l_{\lambda_{irr}} \neq l_{\lambda_{obs}}$, are calculated as $A_{tot}^{\lambda_{irr}/\lambda_{irr}}(t) \times \frac{l_{\lambda_{irr}}}{l_{\lambda_{obs}}} = \left(C_{NIF}(t) \times \varepsilon_{NIF}^{\lambda_{irr}} + C_{PP}(t) \times \varepsilon_{PP}^{\lambda_{irr}}\right) \times l_{\lambda_{irr}}$.

The solution of the differential equation Eq.1 is considered here for the three possible irradiation situations.

In the case where the irradiation was performed at a wavelength where only NIF absorbs, Eq.1 has been integrated in a closed-form (Maafi and Brown, 2007; Maafi and Brown, 2008; Maafi, 2010) and leads to the following integrated rate-law, expressing the temporal variation of the observed absorbance ($A_{NIF}^{\lambda_{irr}/\lambda_{obs}}(t) = C_{NIF}(t) \times \varepsilon_{NIF}^{\lambda_{obs}} \times l_{\lambda_{obs}}$):

$$A_{NIF}^{\lambda_{irr}/\lambda_{obs}}(t) = \frac{l_{\lambda_{obs}}}{l_{\lambda_{irr}}} \times Log\left[1 + \left(10^{\left(A_{tot}^{\lambda_{irr}/\lambda_{irr}}(0) \times \frac{l_{\lambda_{irr}}}{l_{\lambda_{obs}}}\right)} - 1\right) \times e^{-k_{NIF}^{\lambda_{irr}} \times t}\right] \qquad (Eq.3)$$

with $A_{NIF}^{\lambda_{irr}/\lambda_{obs}}(0)$ and $A_{NIF}^{\lambda_{irr}/\lambda_{obs}}(t)$ being the absorbances of NIF at the initial and at a given time t, respectively. $k_{NIF}^{\lambda_{irr}}$ is the overall unimolecular photoreaction rate-constant, given by

$$k_{NIF}^{\lambda_{irr}} = \Phi_{NIF \to PP}^{\lambda_{irr}} \times \varepsilon_{NIF}^{\lambda_{irr}} \times l_{\lambda_{irr}} \times P_{\lambda_{irr}} \times Ln(10) \qquad (Eq.4)$$

For an isosbestic irradiation (where λ_{irr} is equal to that of an isosbestic point, λ_{isos}), the photokinetic factor is constant throughout reaction time (since $A_{tot}^{\lambda_{isos}/\lambda_{isos}}(t)$ is constant, Eq.6). The solution of Eq.1 shows that the kinetics obeys a monoexponential rate-law (Maafi and Brown, 2005),

$$A_{tot}^{\lambda_{isos}/\lambda_{obs}}(t) = A_{tot}^{\lambda_{isos}/\lambda_{obs}}(0) + \left(A_{tot}^{\lambda_{isos}/\lambda_{obs}}(0) - A_{tot}^{\lambda_{isos}/\lambda_{obs}}(\infty)\right) \times \left(e^{-k_{NIF}^{\lambda_{isos}} \times t} - 1\right) \quad (Eq.5)$$

With $A_{tot}^{\lambda_{isos}/\lambda_{obs}}(\infty)$ is the absorbance of the medium after a long reaction time. The overall rate-constant is given by

$$k_{NIF,PP}^{\lambda_{isos}} = \Phi_{NIF\rightarrow PP}^{\lambda_{isos}} \times \varepsilon_{NIF}^{\lambda_{isos}} \times l_{\lambda_{isos}} \times P_{\lambda_{isos}} \times F_{\lambda_{isos}} \qquad (Eq.6)$$

$F_{\lambda_{isos}}$ is calculated by Eq.2 where the absorbance is that of the isosbestic point $A_{tot}^{\lambda_{isos}/\lambda_{isos}}(t)$

However, if the irradiation is performed at a non-isosbestic wavelength where both species absorb, i.e. where $F_{\lambda_{irr}}$ involves $A_{tot}^{\lambda_{irr}/\lambda_{irr}}(t) = A_{NIF}^{\lambda_{irr}/\lambda_{irr}}(t) + A_{PP}^{\lambda_{irr}/\lambda_{irr}}(t)$, Eq.1 cannot be integrated in a closed-form and the integrated rate law for this case has, thus far, not been established. We propose here for the first time the following semi-empirical equation to describe the kinetics of NIF in the above conditions,

$$A_{tot}^{\lambda_{irr}/\lambda_{obs}}(t) = A_{tot}^{\lambda_{irr}/\lambda_{obs}}(\infty) + \frac{A_{NIF}^{\lambda_{irr}/\lambda_{obs}}(0) - A_{tot}^{\lambda_{irr}/\lambda_{obs}}(\infty)}{A_{NIF}^{\lambda_{irr}/\lambda_{irr}}(0) - A_{tot}^{\lambda_{irr}/\lambda_{irr}}(\infty)} \times \frac{l_{\lambda_{obs}}}{l_{\lambda_{irr}}}$$
$$\times Log\left[1 + \left(10^{\left[\left(A_{NIF}^{\lambda_{irr}/\lambda_{irr}}(0) - A_{tot}^{\lambda_{irr}/\lambda_{irr}}(\infty)\right) \times \frac{l_{\lambda_{irr}}}{l_{\lambda_{obs}}}\right]} - 1\right) \times e^{-k_{NIF}^{\lambda_{irr}} \times t}\right] \qquad (Eq.7)$$

with $A_{tot}^{\lambda_{irr}/\lambda_{irr}}(\infty) = C_{NIF}(0) \times \varepsilon_{PP}^{\lambda_{irr}} \times l_{\lambda_{obs}}$ and the photoreaction overall rate-constant being expressed as

$$k_{NIF}^{\lambda_{irr}} = \Phi_{NIF\rightarrow PP}^{\lambda_{irr}} \times \varepsilon_{NIF}^{\lambda_{irr}} \times l_{\lambda_{irr}} \times P_{\lambda_{irr}} \times F_{\lambda_{irr}}^{PP} \qquad (Eq.8)$$

243 with $F_{\lambda_{irr}}^{PP}$ the photokinetic factor (Eq.2) calculated using the absorbance of the photoproduct at
244 the irradiation wavelength at the end of the reaction, i.e. $A_{tot}^{\lambda_{irr}/\lambda_{irr}}(t)$ in Eq.2 is made equal to
245 the constant $A_{tot}^{\lambda_{irr}/\lambda_{irr}}(\infty)$.

246

247 *3.2. NIF photoreaction*

248

249 The photoconversion of NIF leads to a nitroso (PP) derivative (Piechocki and Thoma, 2010;
250 Tonnesen, 2004; Albini and Fasani, 1998; Pietta et al., 1981; Fasani et al., 2006; Gorner, 2010)
251 according to Scheme 1. Albini and Fasani (1998) reported that the nitroso derivative might be
252 converted into a nitro derivative through a thermal re-oxidation. Subsequent results from the
253 same team (Fasani et al., 2006) concluded to the uniqueness of the photoproduct (as the nitroso
254 derivative) regardless of the presence and the absence of oxygen. A similar conclusion has
255 been reached by other studies (Gorner, 2010; Fasani et al., 2008). This however does not
256 support the suggestion of Majeed et al. (1987) that the nature of the product generated during
257 NIF photoreaction, is wavelength-dependent. In any case, it is clear that the monochromatic
258 photodegradation of NIF leads to a unique photoproduct. The progress of the reaction is
259 indicated by the changes taking place on the absorption spectra where some absorption maxima
260 appear and others disappear (Fig.1). The overall time for NIF depletion in our experimental
261 conditions was *c.a.* 1000 s.

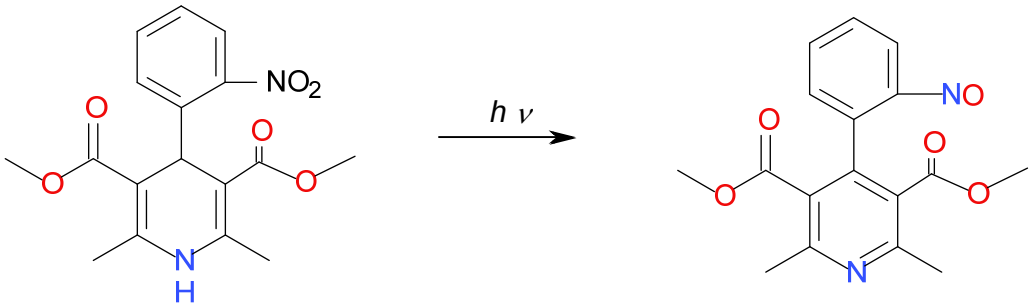

NIF PP

262

263 **Scheme 1**: Phototransformation of Nifedipine.

264

265

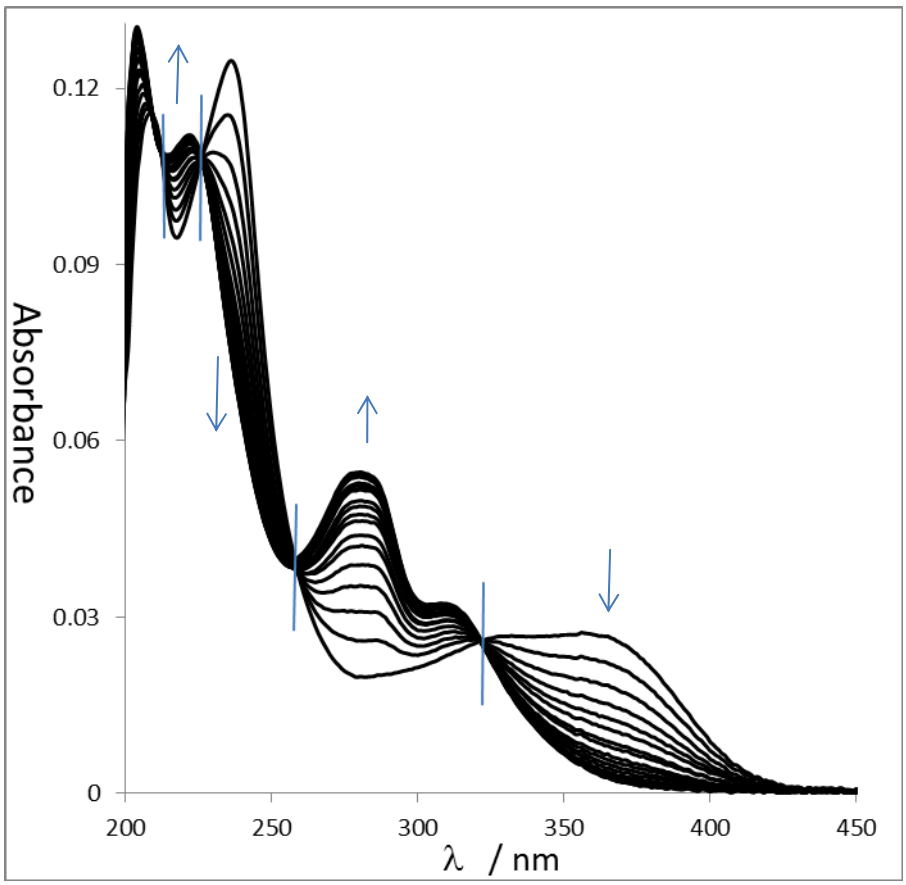

266

267 **Figure 1**: Evolution of the electronic absorption spectra of 5.14 x 10^{-6} M NIF ethanolic
268 solution subjected to a continuous irradiation with a 390-nm monochromatic beam (total
269 irradiation time of 1.2 x 10^{3} s at a radiant power of P_{390} = 9.26 x 10^{-7} einstein.s^{-1}.dm^{-3}). The
270 arrows indicate the direction of the evolution of absorption maxima during photoreaction
271 and vertical lines cross the spectra at the isosbestic points.

3.3. NIF quantum yields at different wavelengths

The kinetic traces were fitted to the model (Fig.2) and the corresponding quantum yields were worked out from the values of the corresponding overall reaction rate-constant (obtained from the fitting $k_{NIF}^{\lambda_{irr}}$) and Eqs. 4, 6 or 8. The results shown in Fig.2 and Table 1, overall indicate that the photochemical quantum yield of NIF increases with increasing irradiation wavelength. The value obtained with λ_{irr} = 321 and 370 nm (Table 1) respectively agree with those determined in 2-propanol and methanol ($\Phi_{NIF\rightarrow PP}^{313}$ = 0.30 and 0.33, respectively) at 313 nm using a method based on Aberchrome (Gorner, 2010), and in acetonitrile and methanol ($\Phi_{NIF\rightarrow PP}^{366}$ = 0.27 – 0.35 and $\Phi_{NIF\rightarrow PP}^{254}$= 0.23 – 0.24, respectively) with irradiation beams of a 35-nm bandwidth centred at 366 and 254 nm using HPLC data corresponding to only 25 % depletion of NIF (Fasani et al., 2008).

Our results show that there is a significant difference between irradiation of the first and second NIF absorption regions (200 – 280, and 300 – 400 nm, respectively, Table 1). NIF reactivity to irradiation in the UVC – UVB regions is much more moderate than that observed under UVA irradiation.

The quantum yield values (Table 1) almost triple between 282 and 370 nm. This strongly suggests that the photodegradation of NIF is mainly due to UVA and visible radiations.

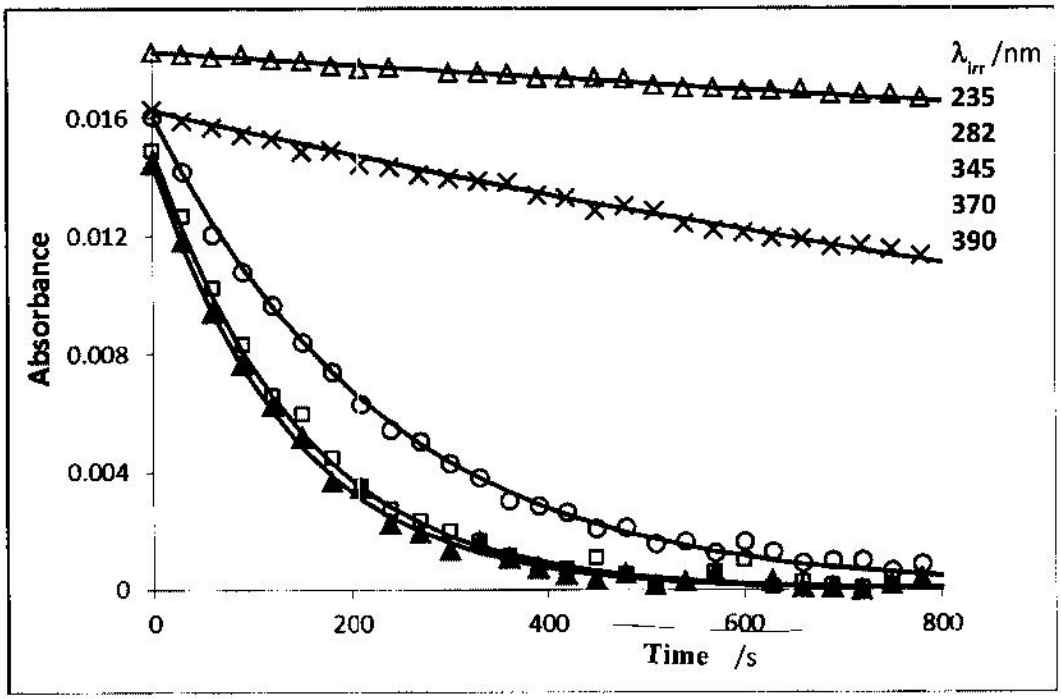

Figure 2: Photokinetic experimental traces of nifedipine in ethanol, observed at λ_{obs} = 390 nm and subjected to continuous irradiation with monochromatic light beams at λ_{irr} = 235, 282, 345, 370 and 390 nm, (labelled with Δ, x, O, □ and ▲, respectively). The experimental data were fitted to the model Eqs.3, 5 or 7 (lines).

Table 1: Quantum yield and overall reaction rate-constant values of NIF for a set of monochromatic irradiations.

λ_{irr}	$A_{NIF}^{\lambda_{irr}/390}(0)$	$P_{\lambda_{irr}}$ $/einstein.s^{-1}.dm^{-3}$	$k_{NIF}^{\lambda_{irr}} \times 10^3$ /s^{-1}	$\Phi_{NIF\rightarrow PP}^{\lambda_{irr}}$
390	0.0151	9.11 x 10^{-7}	7.50	0.509
370	0.0263	7.67 x 10^{-7}	7.20	0.322
345	0.0248	4.37 x 10^{-7}	4.05	0.305
321	0.0261	3.18 x 10^{-7}	2.36	0.267
282	0.0162	1.88 x 10^{-7}	0.440	0.109
250	0.0142	1.50 x 10^{-7}	0.265	0.025
235	0.0182	2.36 x 10^{-7}	0.135	0.004
223	0.0144	2.98 x 10^{-7}	0.180	0.0057

3.4. Effect of NIF concentration on the photodegradation rate-constant

The kinetic traces obtained at an observation wavelength of $\lambda_{obs} = 390$ nm were fitted to the adequate model equation (either Eq. 3, 5 or 7). For the set of concentrations used, good agreements were generally found between the experimental data and the kinetic models (Fig.3). The determined rate-constants are presented in Table 2.

In the cases where the irradiation is carried out at wavelengths where both species absorb (including irradiation at an isosbestic point), a decrease of NIF photodegradation overall rate-constant is observed. Whereas, no significant differences were observed on the values of $k_{NIF}^{\lambda_{irr}}$ for irradiations at 390 nm (where only NIF absorbs).

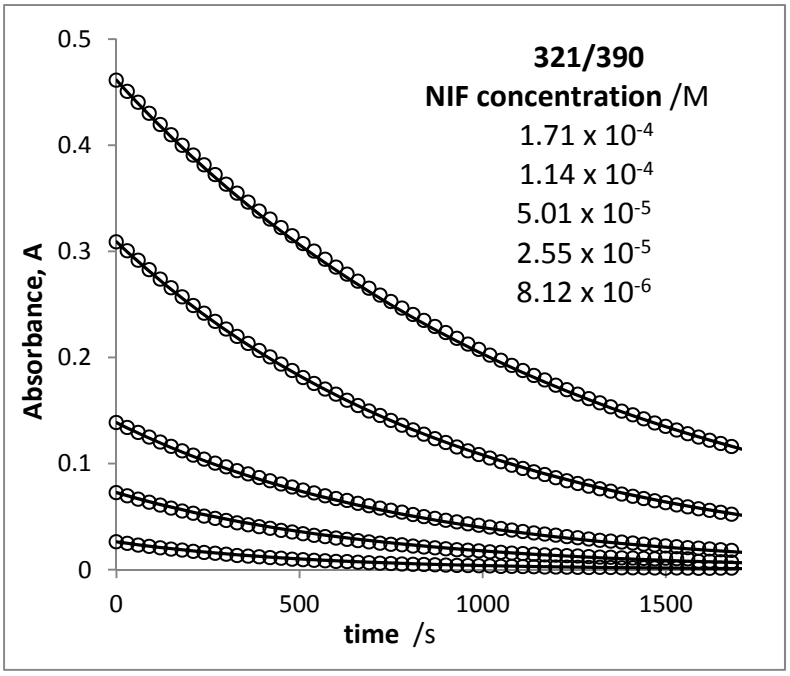

Figure 3: Photokinetic traces of NIF ethanolic solutions of various concentrations (1.7×10^{-4} – 8.1×10^{-6} M). Irradiation at the isosbestic point 321 nm and observation at 390 nm (321/390).

Table 2 : Initial concentrations and overall rate-constants of NIF photodegradation measured at various irradiation wavelengths.

λ_{irr}	$A_{NIF}^{\lambda_{irr}/390}(0)$	$k_{NIF}^{\lambda_{irr}}$ /s	$C_{NIF}(0) \times 10^5$ /M
281	0.277	0.00009	10.2
	0.146	0.00022	5.28
	0.068	0.00039	2.37
321	0.461	0.00082	17.1
	0.309	0.000105	11.4
	0.073	0.000141	2.56
354	0.144	0.00389	5.21
	0.069	0.00414	2.41
	0.027	0.00430	0.84
390	0.129	0.00482	4.65
	0.070	0.00483	2.44
	0.028	0.00489	0.87

3.5. NIF actinometric potential

As it has been shown above, the quantum yield of NIF in the UVA-visible spectral region is overall higher than those recorded in the UVB and UVC ranges. Owing to the radiant power capacity of our experimental set up, only irradiation in the UVA-visible region (λ_{irr} = 321, 345, 370 and 390 nm) is suitable for a quantitative actinometric investigation.

The photokinetic model equations (Eqs.3, 5 and 7) fitted NIF experimental traces with good accuracy (Fig.4), confirming that they closely describe the evolution of the photoreaction for the selected radiant power values. This observation corroborates the aforementioned results regarding the unimolecular mechanism of NIF photodegradation (Scheme 1).

The overall reaction rate-constants ($k_{NIF}^{\lambda_{irr}}$) determined for each curve were plotted against the corresponding radiant power values ($P_{\lambda_{irr}}$) for each selected irradiation wavelength. $k_{NIF}^{\lambda_{irr}}$ values spanned the range 7 x 10^{-4} to 7.5 x 10^{-3} s^{-1}. Straight lines were obtained with squared correlation coefficients (r) over 0.98 and intercepts close to zero (Table 3).

The overall rate-constant equation (Eq. 8) can be rearranged as a function of the radiant power as,

$$k_{NIF}^{\lambda_{irr}} = \Phi_{NIF\rightarrow PP}^{\lambda_{irr}} \times \varepsilon_{NIF}^{\lambda_{irr}} \times l_{\lambda_{irr}} \times F_{\lambda_{irr}}^{PP} \times P_{\lambda_{irr}} = \beta_{\lambda_{irr}} \times P_{\lambda_{irr}} \qquad (Eq.9)$$

where the coefficient $\beta_{\lambda_{irr}}$ is a constant for a given set of irradiation wavelength, initial NIF concentration and optical path length of irradiation (Table 3).

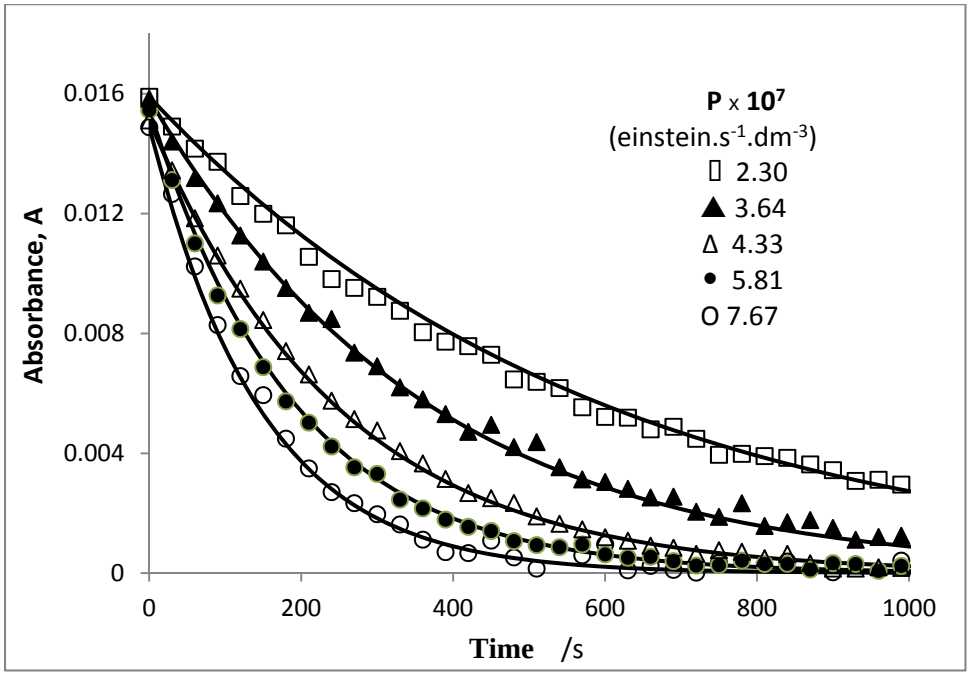

Figure 4: Effect of increasing radiant power on NIF kinetic traces. Irradiation/observation wavelengths were 370/390.

Table 3 : Correlation equations for the variation of NIF photodegradation rate-constants ($k_{NIF}^{\lambda_{irr}}$) with radiant power ($P_{\lambda_{irr}}$), and the corresponding $\beta_{\lambda_{irr}}$ factors determined at various irradiation wavelengths.

Irradiation wavelength λ_{irr} / nm	Equation of the line $k_{NIF}^{\lambda_{irr}} = \beta_{\lambda_{irr}} \times P_{\lambda_{irr}} + intercept$	Correlation coefficient r^2	$P_{\lambda_{irr}} \times 10^7$ einst.s^{-1}.dm^{-3}
390	$8489.2 \times P_{390} - 3 \times 10^{-4}$	0.993	2.87 – 9.11
370	$9775.9 \times P_{370} + 2 \times 10^{-4}$	0.988	2.30 – 7.37
345	$8116.9 \times P_{345} + 4 \times 10^{-4}$	0.987	2.39 – 5.19
321	$9131.8 \times P_{321} - 3 \times 10^{-4}$	0.997	1.20 – 3.46

3.6. Effect of TRZ, SSY and QY concentrations on NIF photoreaction rate-constant

The electronic absorption spectra of the dyes (TRZ, SSY and QY) are characterised by two broad absorption regions situated in the 200 – 320 nm and 320 – 550 nm. Since these features overlap with those of NIF, each dye is potentially capable of photoprotecting NIF especially from UVA and visible radiations (Rowe, 2003). These dyes are found to be photostable when individually tested in the same experimental conditions used for NIF.

Increasing concentrations of a given dye in NIF solution has the effect of gradually reducing the photodegradation reaction of the dihydropyridine derivative. The data are reported on Table 4. Fig.5 shows the traces of NIF obtained with an irradiation and observation at 390 nm for SSY concentrations ranging from 1.14 x 10^{-5} M to 5.35 x 10^{-5} M. NIF photostability improvements in the dyes' presence confirm similar results that were observed, usually for one given amount of dye, with curcumin, fast yellow, chrysoine, apocarotinal and cochineal in

366 solution (Thoma and Klimek, 1991), and tartrazine (Teraoka et al., 1988;) and curcumin
367 (Tonnesen, 2001) in film coating materials.

368

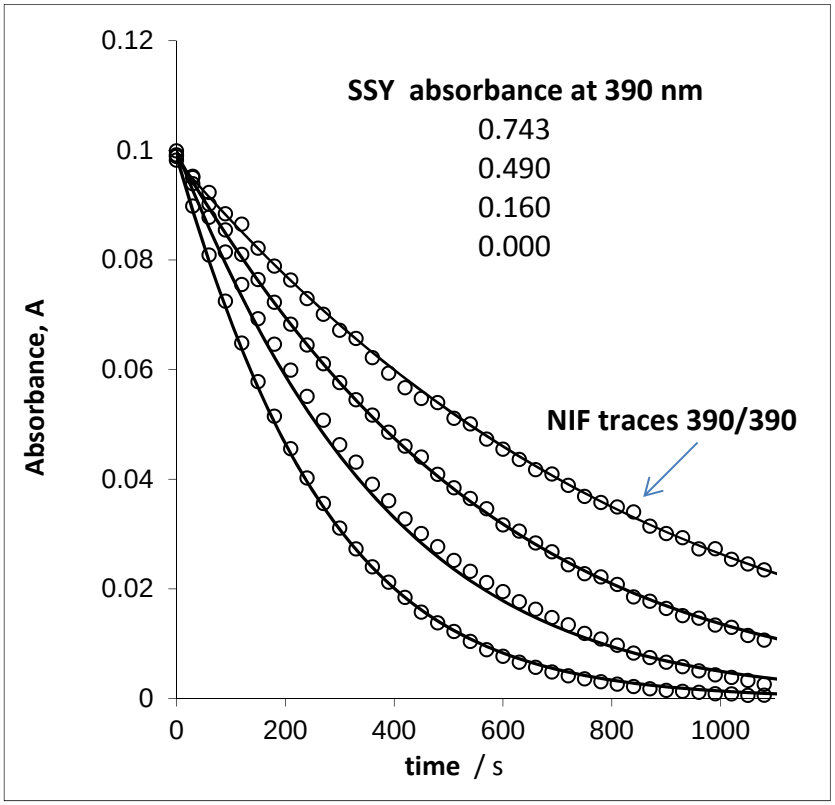

369

370 **Figure 5**: Effect of increasing SSY concentration (1.14×10^{-5} - 5.35×10^{-5} M) on the
371 photodergradation traces (circles) of NIF (3.52×10^{-5} M solutions in ethanol).

372

Table 4:, NIF overall reaction rates and photoreaction reduction percentages in the presence of various excipient-dyes' concentrations.

	Concentration of the dye /M	$A_{dye}^{\lambda_{irr}}$ [a]	$k_{NIF}^{\lambda_{irr}}$ /s^{-1}	$\frac{k_{NIF}^{\lambda_{irr}}\left(A_{dye}^{\lambda_{irr}}=0\right)}{k_{NIF}^{\lambda_{irr}}\left(A_{dye}^{\lambda_{irr}}\neq 0\right)}$	% reduction [b]
NIF [c]	0	0	0.0067	1	0
Tartrazine (TRZ)	1.96×10^{-5}	0.252	0.00430	1.558	33.48
	3.60×10^{-5}	0.518	0.00315	2.127	53.98
	6.43×10^{-5}	0.978	0.00210	3.191	69.22
	8.82×10^{-5}	1.364	0.00164	4.085	74.86
	1.24×10^{-4}	1.948	0.00130	5.154	79.25
Quinoline Yellow (QY)	1.76×10^{-5}	0.319	0.0043	1.558	26.86
	4.03×10^{-5}	0.741	0.0032	2.094	38.80
	5.56×10^{-5}	1.025	0.0026	2.577	47.76
	1.05×10^{-4}	1.940	0.0018	3.722	64.18
Sun set Yellow (SSY)	1.14×10^{-5}	0.160	0.0033	2.030	22.98
	2.32×10^{-5}	0.324	0.0026	2.566	33.58
	3.53×10^{-5}	0.490	0.0022	2.979	38.80
	5.36×10^{-5}	0.742	0.0015	4.351	49.22

[a]: absorbance of the dye measured at the irradiation wavelength of 390 nm.
[b]: the constant concentration of nifedipine was 4.65×10^{-5} M.

[c]: the radiant power value for the experiments performed at an irradiation of λ_{irr} = 390 nm was $P_{390} = 9.5 \times 10^{-7}$ einstein dm^{-3} s^{-1}.

4. DISCUSSION

NIF converts to a nitrosophenylpyridine photoproduct (PP, Scheme 1) under artificial light of any wavelength (Pietta et al., 1981; Fasani et al., 2006; Gorner, 2010) in the nanosecond time span (Gorner, 2010). This photoreaction does not involve a triplet state pathway or a radical course (Fasani et al., 2006), and is insensitive to the presence of oxygen (Fasani et al., 2006; Gorner, 2010). These features were found to be compatible with the occurrence of an intramolecular H-atom transfer (Fasani et al., 2006). The identity of PP has been established by spectroscopic/separation techniques (Piechocki and Thoma, 2010; Tonnesen, 2004; Albini and Fasani, 1998; Pietta et al., 1981; Fasani et al., 2006; Gorner, 2010) and its occurrence as a unique photoproduct was evidenced by multivariate curve analysis (Shamsipur et al., 2003). NIF is thermally stable whereas PP is both thermally and photochemically stable. Therefore, NIF reaction obeys a unimolecular mechanism as proposed in Scheme 1.

The spectrophotometric spectral changes (Fig.1) are attributed to such transformation of NIF. The broad long-wavelength band (λ > 300 nm) belongs to the dihydropyridine chromophore (Krufurst and Kuhan, 1983) which undergoes aromatisation during the photoreaction (Scheme 1). The disappearance of this band is concomitant with the appearance of a series of new peaks between 200 and 300 nm. Therefore, the absorption spectra of NIF completely overlaps that of PP, whereas, the spectral region beyond *c.a.* 370 nm corresponds exclusively to the absorption of the mother compound.

Generally, the adopted description of the kinetic behaviour or the fitting of the experimental traces of NIF and many other drugs, has mostly been based on a first-order kinetics treatment often using chromatographic data relative to the initial species (Sangoi et al., 2013; Mattos et al., 2012; Piechocki and Thoma, 2010; Tonnesen, 2004; Gorner, 2010; Souza et al., 2010; Glass et al., 2004; Shamsipur et al., 2003; Thoma and Klimek, 1991; Majeed et al., 1987). Even though it has not been comprehensively discussed in the literature, this strategy implicitly amounts to working under the assumption of an isosbestic irradiation as its integrated rate-law, the monoexponential model (Eq.5), is mathematically analogous to the equation used for a first-order kinetic treatment. Such kinetic treatments were employed for many reactions in the literature, despite the fact that most often not only irradiation beam was non-isosbestic, was absorbed by more than one species (mother compound and its photoproducts) but also it usually is polychromatic (Piechocki and Thoma, 2010; Tonnesen, 2004; Gorner, 2010; Souza et al., 2010; Glass et al., 2004; Shamsipur et al., 2003; Thoma and Klimek, 1991; Majeed et al., 1987). Furthermore, when the first-order kinetic treatment is employed, the overall rate-constant of the photoreaction (k), obtained from fitting the given experimental trace, is usually numerically defined by a given value but the analytical expression of this constant is not accessible through this treatment. Hence, there is no explicit relationship linking the determined overall rate-constant to the fundamental parameters of the photoreaction (such as the reaction quantum yield).

It has also been shown that in some cases, such as those of Benzydamine hydrochloride and ketrolac thromethamine (Piechocki and Thoma, 2010), the photodegradation reaction data can be equally well fitted by either first- or zero-order kinetics.

427 Accordingly, it becomes evident that fitting mother compound traces with a first-order kinetic
428 model is a mere approximation in most cases.

429

430 In this respect, a previous study (Maafi and Brown, 2007) has shown that the monoexponential
431 model does not fit well the data of a species subjected to monochromatic non-isosbestic
432 irradiation. This conclusion holds as well when the data correspond to the cumulative
433 absorbance of the mother compound and its photoproduct.

434

435 The occurrence of discrepancies between the first-order kinetics and experimental data might
436 have been at the origin of another proposal. Here, the fitting of the complete kinetic trace of
437 NIF is performed by a two-stage treatment using the thermal kinetic models corresponding to a
438 zero-order reaction up to the half-life time, followed by an exponential first-order equation for
439 the rest of the traces. This approach has been applied to kinetic data obtained either in solution
440 (Piechocki and Thoma, 2010; Tonnesen, 2004; Albini and Fasani, 1998; Shamsipur et al.,
441 2003) or in the solid state (Piechocki and Thoma, 2010; Tonnesen, 2004; Albini and Fasani,
442 1998).

443

444 As an illustration example, we applied this two-stage treatment to our 390/390 trace of NIF in
445 ethanol as shown in Fig.6.

446

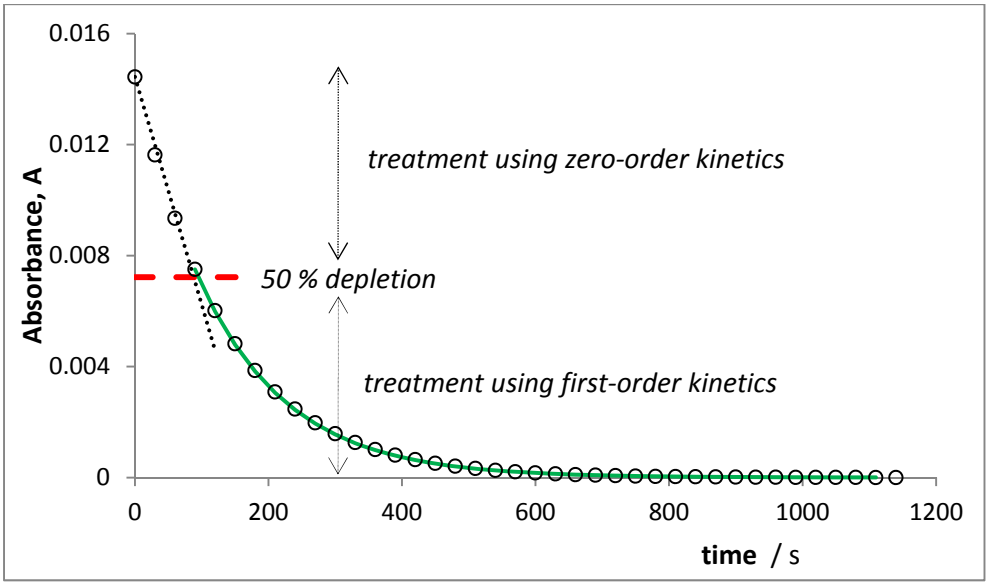

Figure 6: Application of the two-stage treatment proposed in the literature to the photokinetic traces of 3.88×10^{-6} M nifedipine in ethanol subjected to continuous irradiation with a monochromatic 390 nm-light beam (P_{390} = 9.11 10^{-7} einstein s^{-1} dm^{-3}), and observation at 390 nm. Experimental data (circles) were fitted to the zero-order (straight dotted line) and first-order (plain line) kinetic models. The horizontal dashed line indicates the 50 % depletion limit.

Despite the usual good fitting of the data as observed in Fig.6, this two-stage treatment approach falls short to justify or explain the physical/chemical reasons behind the change in the reaction order that is supposed to occur in the course of the photoreaction. In addition, the meaning, the analytical expressions and/or the relationship between the rate-constants obtained for the different reaction stages, corresponding to separate segments of the trace, were not clarified.

While the above approaches may find use in the comparison of the variation of the rate-constants of the initial stages of NIF-photoreactions (e.g. the slope of the zero-order kinetics)

464 performed in the same experimental and irradiation conditions, it cannot be used for
465 quantitative analysis to compare different studies.

466

467 Despite such limitations, the above approaches as well as a number of similar strategies are still
468 usually employed in the treatments of the kinetic data of drugs' photoreactions (Sangoi et al.,
469 2013; Mattos et al., 2012; Piechocki and Thoma, 2010; Tonnesen, 2004; Albini and Fasani,
470 1998; Glass et al., 2004). It seems that the main reason behind this situation is the lack of
471 integrated rate-law models that are able to describe photoreactions with the same mathematical
472 rigour to those describing thermal reactions. The shortage in integrated rate-law models for
473 photoreactions is itself primarily due to the difficulty to achieve closed-form integration of the
474 differential equations of such reactions (due to the presence of a time-dependent photokinetic
475 factor $F_{\lambda_{irr}}$, Eqs.1 and 2).

476

477 In the present study, a strategy based on irradiation conditions has been primarily devised to
478 deal with the treatment of kinetic data corresponding to any system reacting in a similar
479 manner to that described for NIF in Scheme 1, the so-called unimolecular photoreaction or
480 AB(1Φ) systems.

481

482 When $F_{\lambda_{irr}}$ is constant during the photoreaction time, i.e. when irradiation is performed at an
483 isosbestic wavelength, the solution for the corresponding differential equation is worked out
484 through variables separation (as in the case of thermal reaction equations) and leads to a
485 monoexponential law as given by Eq.5 (Maafi and Brown, 2005).

In a previous study (Maafi and Brown, 2007), it has been shown that the differential equation of the unimolecular photoreaction, subjected to a non-isosbestic irradiation where only the initial species absorb at the specified irradiation wavelength, can be integrated in a closed-form. The obtained logarithmic solution (Eq.3), similarly to the monoexponential model, is applicable irrespective of the experimental conditions in which the reaction is performed (Maafi, 2010; Maafi and Brown, 2007).

In addition to the aforementioned cases, one must consider the situation where the reaction species (NIF and PP) absorb differently at the non-isosbestic irradiation wavelength (λ_{irr}), which represents the most general irradiation situation. Unfortunately thus far, the differential equation of this reaction case (even though it is not considerably mathematically different from those of the latter cases) cannot be integrated in a closed-form. In addition, the latter models (Eqs. 3 and 5) are not suitable to fit the data of this third case. Thus, in order to complete the set of equations describing AB(1Φ) kinetics, we propose here a semi-empirical rate-law model (Eq.7) for this third case.

The validity of Eq.7 has been tested on synthetic data generated with a fourth-order Runge-Kutta (RK) method. The calculated RK traces can be considered as a faithful representation of reaction kinetics as they can be obtained with high precision (Mauser and Gauglitz, 1998). Hence, for a given reaction system (with particular values for the parameters involved in Eq.1), a synthetic RK trace is calculated and later fitted with Eq.7.

In general a good agreement has been found between the synthetic data and semi-empirical model, Eq.7, for a large number of values adopted for the system parameters $C_{NIF}(0)$, $\Phi_{NIF\rightarrow PP}^{\lambda_{irr}}$, $\varepsilon_{NIF}^{\lambda_{irr}}$, $\varepsilon_{PP}^{\lambda_{irr}}$, $l_{\lambda_{irr}}$, $l_{\lambda_{obs}}$and $P_{\lambda_{irr}}$. This proved that the mathematical form of Eq.7 is adapted to describing the kinetic behaviour of unimolecular photoreactions when subjected to non-isosbestic irradiation where both A and B (e.g. NIF and PP) absorb. However, at this stage it is only possible to determine the value of the overall rate-constant of the reaction ($k_{NIF}^{\lambda_{irr}}$ as a fitting parameter of Eq.7) but not its expression. For the purpose of defining the analytical expression of $k_{NIF}^{\lambda_{irr}}$, we tested a set of 250 RK traces corresponding to different but plausible reaction systems spanning various plausible experimental conditions. Our findings yield the formula of $k_{NIF}^{\lambda_{irr}}$ as given in Eq.8 provided that the value of $F_{\lambda_{irr}}^{PP}$ exceeds the value 1.2 which corresponds to an absorbance of PP at λ_{irr} across l_{irr} of no more than 0.64 at the end of the photoreaction (Fig.7). This condition is not a serious limitation for the usefulness of Eq.7 since it can readily be met by reducing either the initial concentrations of NIF or the optical path length of the irradiation beam inside the sample (l_{irr}). For the situations where $F_{\lambda_{irr}}^{PP} < 1.2$, Eq.7 can generally still be applied but $k_{NIF}^{\lambda_{irr}}$ will only represent a parameter of the fitting because its analytical expression is not precisely defined (*vide infra* discussion on the effects of dyes). It can be useful in comparing the effect of one variable on the rate constant of a given system but cannot be used to compare different systems and/or extract the fundamental parameters of the photodegradation reaction.

The good correlation shown in Fig.7 also supports the efficacy and reliability of the approach, used for the first time in the present study, in unravelling a new semi-empirical integrated rate-law model. The combination of RK synthetic data and a mathematical formulation suitable for

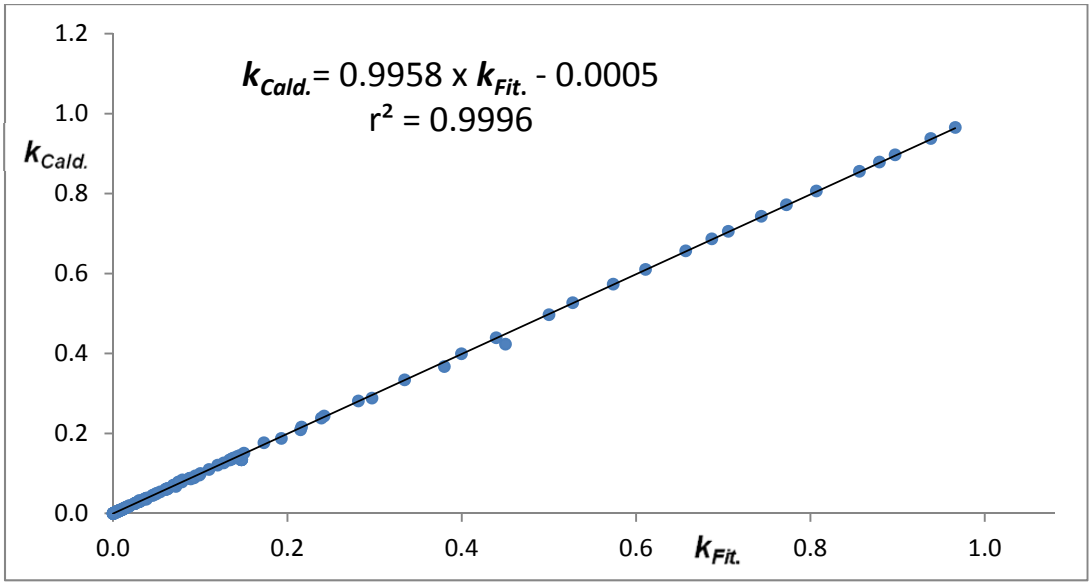

531

532 **Figure 7**: Linear correlation between rate-constants obtained by the fitting of RK data with
533 Eq.7 ($k_{Fit.}^{\lambda_{irr}}$) and those calculated using Eq.8 ($k_{Cald.}^{\lambda_{irr}}$) and parameter values feeding RK
534 calculations.

535

536 AB(1Φ) photodegradations (formulae of the type of Eq.3), has led to the optimization of model
537 Eq.7 and the determination of the expression of its rate-constant. Likewise, this approach might
538 find future applications in developing more semi-empirical rate-law equations for other
539 photodegradation mechanisms and photoactive drug systems whose differential equation
540 cannot be integrated in a closed-form.

541

542 From a general viewpoint, the models presented in this study clearly indicate that the overall
543 rate-constant (Eq.4, 6 and 8) of a unimolecular phototrasformatiom of a drug, such as NIF,
544 depends simultaneously on the reaction quantum yield ($\Phi_{NIF\rightarrow PP}$), the intensity of the radiant
545 light and volume irradiated ($P_{\lambda_{irr}}$), the optical path length of the irradiation light inside the
546 sample (l_{irr}) for all the irradiation cases, and on the final absorption of PP at the irradiation

wavelength ($F_{\lambda_{irr}}^{PP}$ or $F_{\lambda_{isos}}$) when both NIF and PP absorb at λ_{irr}. Hence, the overall rate-constant values cannot directly be indicative of the reaction quantum yield and should not be compared for different irradiation wavelengths or separate experiments, including when the same drug is used, or when the experimental conditions are not identical (i.e. l_{irr}, $P_{\lambda_{irr}}$ and $F_{\lambda_{irr}}^{PP}$). Such values would also be unreliable if polychromatic light is used for irradiation. This reemphasizes the need for a reliable determination of the quantum yield, the only physical quantity that can objectively inform on drugs' photoreactivity and which can be safely used for comparison purposes if obtained with effective monochromatic light.

Besides, it is important to notice that the present approach allows the determination of $\Phi_{NIF\rightarrow PP}$, from the values of $k_{NIF}^{\lambda_{irr}}$ obtained from the fitting, and the corresponding Eq.4, 6 or 8, based on spectrophotometric data without a requirement for a prior separation of the reaction components and/or partial use of the kinetic data (considers the full set of data without a special conditions such as the first 20 % or 50 % (Piechocki and Thoma, 2010; Tonnesen, 2004; Albini and Fasani, 1998) depletion limits for NIF).

It is worth noting here that the mathematical formulation of Eq.3, differs considerably from the classical integrated rate-laws describing zero-, first- and second-order kinetics as obtained for thermal reactions. This clearly indicates that photoreactions would not be well described by the latter equations. The exception of the first-order equation for thermal reactions that might be used with data generated for isosbestic irradiation (Eq.5) remains limited with a restricted application due to the fact that isosbestic irradiation concerns quite a narrow section of the drug's spectrum (literally a few individual wavelengths, e.g. four for NIF as shown in Fig.1).

570 Such a situation leads to questions about the meaning of a photochemical reaction's order and
571 whether it is at all possible to establish one. Indeed, not only the integrated rate-law of a pure
572 photoreaction (Eq.3) is mathematically different from the corresponding thermal ones but also
573 the order of the photoreaction cannot be worked out in a classical way from the rate law (Eq.1)
574 due to the presence of a term in the photokinetic factor that holds the concentration as a power
575 of ten. Therefore, it is reasonable to conclude that the simplest AB(1Φ) photoreaction clearly
576 obeys a new and specific order that has not been described before for any known reaction. Its
577 integrated rate-law has the general form depicted in Eq.7. Thus, we propose to call the kinetics
578 obeyed by a unimolecular photochemical reaction of the AB(1Φ) type, as the "*Φ-order*
579 *kinetics*". Work is ongoing in our team to evaluate whether the degradation of the mother
580 compound involved in more elaborate mechanisms still obey the Φ-order kinetics.

581

582 The application of Eqs.3, 5 and 7 to our experimental data showed that NIF kinetics is well
583 described by these models (Fig. 2). NIF photoconversions have been found to obey the models
584 whatever the irradiation and/or the observation wavelength. This indicates that NIF and PP are
585 involved in a unimolecular reaction, confirming the proposed mechanism of Scheme 1. This
586 result corroborates the conclusions obtained by HPLC (Fasani et al., 2006, Gorner, 2010) and
587 multivariate curve analysis (Shamsipur et al., 2003). However, the present kinetic approach has
588 the advantage to be much faster and simpler to implement.

589

590 Photoreaction quantum yields of NIF for a set of irradiation wavelengths (Table 1 and Fig.2)
591 showed that UVA-Vis unlike UVB radiations are mostly responsible for NIF photodegradation
592 (causative wavelength range situated between 300 and 390 nm). The variation of quantum
593 yield values against irradiation wavelength spans the range 0.004 – 0.51. The significant

difference between the two radiation regions agrees with the qualitative conclusion previously reached by comparing photoreaction first-order rate-constants (Thoma and Klimek, 1991). Our results for long wavelengths agreed with those reported in the literature in methanol, 0.24 at λ_{irr} = 254 nm (Fasani et al., 2008), in acetonitrile, 0.27 at λ_{irr} = 366 nm (Fasani et al., 2008), and in water, 0.32 at λ_{irr} = 313 nm (Gorner, 2010).

The differences between our quantum yield values in UVA and UVB regions correlate well with the differences in electronic absorptions of nitrobenzene and hydropyridine moieties (Fasani et al., 2008). If this hypothesis is considered, then our results may emphasise the essential and specific role of the excited-state of the hydropyridine group in the H-transfer mechanism.

The variation of the quantum yield values between 210 and 370 nm with irradiation can be modelled by a sigmoid function (Eq.9) that is only dependent on the irradiation wavelength (Fig.7), as

$$\Phi_{\mathrm{NIF\rightarrow PP}}^{\lambda_{\mathrm{irr}}} = \frac{0.3317}{1 + 57.3684 \times e^{-0.0547(\lambda_{irr}-223)}} \qquad (Eq.9)$$

The agreement between the sigmoid curve and our data is indicated by the linear relationship of the experimental *vs.* calculated quantum yield values that have been obtained from Eq.9 (inset in Fig.8, with and intercept close to zero, a slope and a correlation coefficient close to unity). Therefore, the sigmoid model (Eq.9) facilitates the estimation of NIF quantum yield values in ethanol at any useful wavelength.

615 The sigmoid variation of $\Phi_{NIF\rightarrow PP}^{\lambda_{irr}}$ with irradiation wavelength also indicates that when a
616 polychromatic light (as that of a filtered light of bandwidths of 25 – 50 nm) is used, only
617 approximations/averages of the quantum yield can be obtained that will probably not achieve a
618 comprehensive picture of NIF photoreactivity at a specific wavelength.

619

620

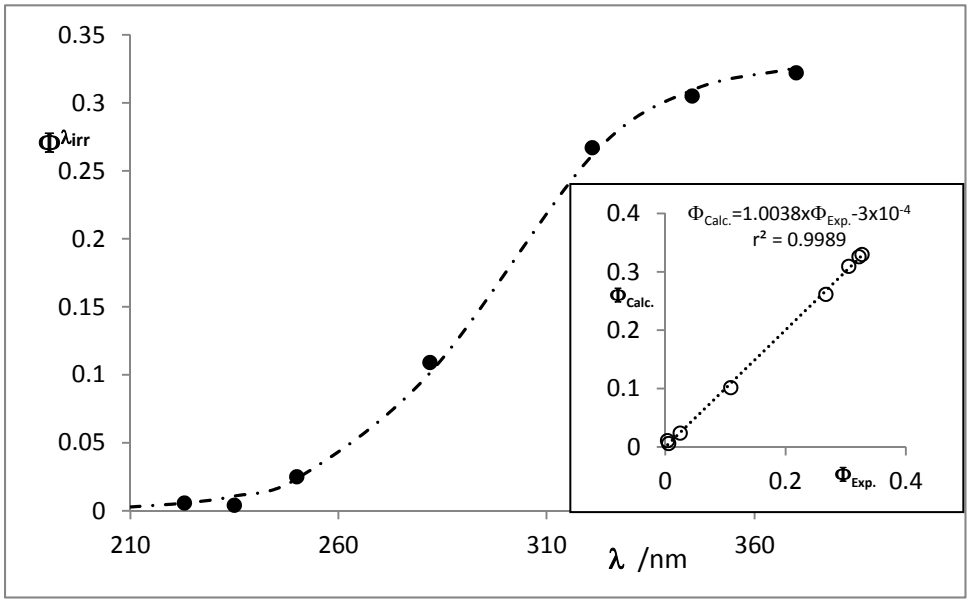

621

622 **Figure 8**: Variation of NIF quantum yield values with irradiation wavelength. Inset : calculated
623 ($\Phi_{Calc.}$, using Eq.9) versus experimental ($\Phi_{Exp.}$) quantum yield values.

624

625 The regular decrease of the photoreaction rate-constant with increasing NIF concentration (Fig.
626 3, Table 2) is consistent with our kinetic models (Eq. 5 and 7). A linear correlation between
627 $k_{NIF}^{\lambda_{irr}}$ and $F_{\lambda_{irr}}$ is in fact implicitly conveyed by the photokinetic factor expressions Eqs.6 and
628 8. Eq.4, however, states that the photoreaction rate-constant is concentration-independent. Our
629 experimental results confirm these theoretical predictions as shown in Fig.9. A 6.2-fold
630 increase of NIF concentration has represented up to *c.a.* 58 % decrease in the value of the
631 photoreaction rate-constant (obtained for an irradiation at the 321-nm isosbestic point). This

clearly indicates that the reaction can undergo a significant slowdown due to increasing NIF initial concentration. This concentration induced slowdown may represent a basis to rationalise a number of qualitative data reported in the literature, which indicated as a general rule, less photodegradation at high NIF concentrations (Piechocki and Thoma, 2010; Tonnesen, 2004) but this observation has never been rationalized mathematically.

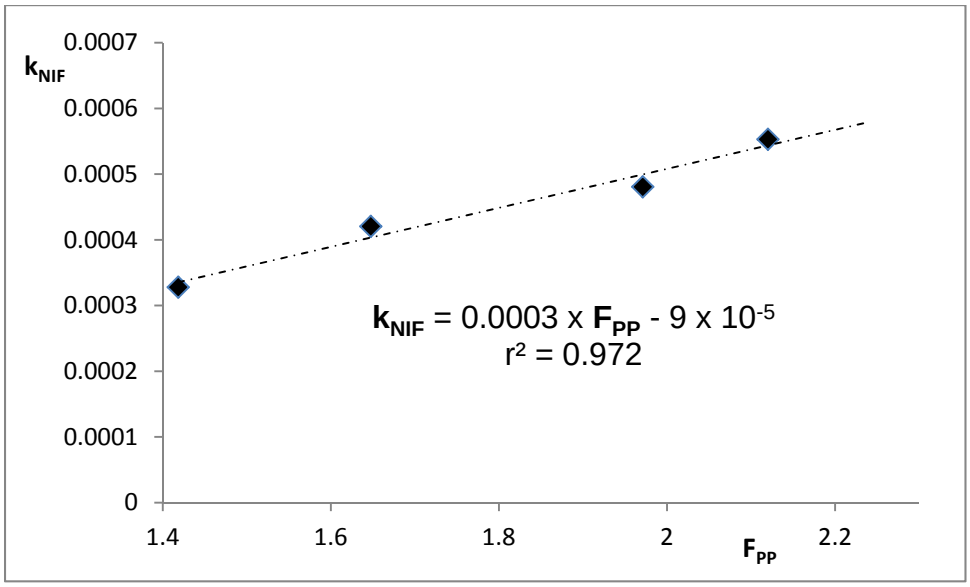

Figure 9: A linear relationship is found between the rate-constant of NIF photodegradation and the photokinetic factor of the product.

This interpretation may also hold for more complex mechanisms where more than one photoproduct species absorb at the irradiation wavelength since the differential equations of photochemical reactions should always involve a photokinetic factor and therefore *a priori* for any system the rate-constants are likely to be concentration-dependent. But most importantly one can deduce that higher concentrations of NIF substantially increase its photostability in the region where NIF and PP absorb. The occurrence of both high concentration and low quantum yield in the region below 300 nm expands the gain in photostability. Nonetheless, this also

649 means that for this type of molecules, it is a requirement to protect the drug from light in the
650 spectral range where only the photoreactive species, NIF, absorbs (at UVA and visible
651 radiations).

652

653 The model Eqs.3, 5 and 7 can also find application in improving actinometric methods of
654 useful drugs. This might be relevant since in terms of measurement of light intensity, there are
655 only a few drugs that have been proposed as actinometers (Piechocki and Thoma, 2010; Kuhn
656 et al., 2004; Dhuna et al., 2008). The ICH recommended actinometer, quinine
657 monohydrochloride, has been found to present a number of drawbacks (Azevedo Filho et al.,
658 2011; Baertschi et al., 2010; Thatcher et al., 2001; Baertschi, 1997).

659

660 In a previous study, it has been shown that an actinometric method based on Eq.4 can be
661 developed for unimolecular photoreactions but it was only applicable if one species absorbed
662 (and reacted) in the medium (Maafi, 2010). This corresponds to the 360 – 400 nm spectral
663 region of NIF.

664

665 The equation model proposed in this study (Eq.7) offers the possibility of devising a method
666 for wavelength regions where both the species involved in the unimolecular reaction absorb.
667 The combination of all the models proposed in this study, Eqs. 3, 5 and 7 is expected to allow
668 developing actinometers for the whole absorption (UV and Vis) range of any species obeying a
669 unimolecular photoreaction. Here, the photochemical behaviour of NIF was used to prove this
670 principle.

671

672 Our results (Table 3 and Fig.4) show clearly that NIF can be used as an actinometer for given
673 wavelengths, provided that the adequate model equation is used (either Eq.3, 5 or 7). The linear
674 relationships between $k_{NIF}^{\lambda_{irr}}(m)$ and $P_{\lambda_{irr}}(m)$, for the "*m*" values of the radiant power with
675 each selected λ_{irr}, are characterised by correlation coefficients close to unity and intercepts
676 approaching zero values.

677

678 The variation recorded between $\beta_{\lambda_{\mathrm{irr}}}$ factors (Table 3) is due to the fact that these factors
679 depend on a number of quantities (i.e. the irradiation wavelength, NIF initial concentration, the
680 optical path length, the absorption coefficients of the species and the quantum yield at the
681 irradiation wavelength) which may differ from one wavelength to the other.

682

683 From a practical point of view, the unknown radiant power of a given light source at a
684 particular irradiation wavelength can be obtained by fitting the experimental kinetic data of the
685 reaction at hand, obtained using a monochromatic beam between 220 – 400 nm from this given
686 light source, to the appropriate model equation (either Eq.3, 5 or 7) and determining the overall
687 rate-constant of NIF photodegradation. The obtained $k_{\mathrm{NIF}}^{\lambda_{\mathrm{irr}}}$ value will then be divided by the
688 corresponding $\beta_{\lambda_{\mathrm{irr}}}$ factor to give the actual value of the unknown $P_{\lambda_{\mathrm{irr}}}$.

689

690 It is interesting to notice that this method can *a priori* be applied to any radiant power values
691 (as confirmed by our RK tests) and can be extended to any drug as long as its mechanism
692 obeys unimolecular kinetics. This means that there is potential to develop a series of
693 actinometers for weak radiant power sources (using highly reactive drugs such as NIF for

694 λ_{irr} > 300 nm) and other drugs for light sources delivering higher energy beams (using slow
695 photodegradable drugs, e.g. NIF for λ_{irr} < 300 nm). This might help in proposing alternatives
696 to quinine actinometry. It may also prove interesting to consider the possibility of a series or a
697 set of actinometer-drugs to cover the widest possible radiation range. The useful spectral
698 section of NIF (280 – 400 nm) can be completed by other drugs (or chemicals) on both sides
699 for that region (as is the case, if we consider 1,2-bis[2-methylbenzo[b] thiophen-3,3,4,4,5,5-
700 hexafluoro-1-cyclopentene for the visible 405 – 570 nm region (Maafi, 2010)).

701

702 In this context however, there is a need to address the important issue related to future
703 developments of new actinometric methods that would be useful for polychromatic light since
704 the present method is only appropriate for monochromatic radiations.

705

706 On the other hand, since $\beta_{\lambda_{irr}}$ depends on the initial concentration via the variation of the
707 photokinetic factor, $F_{\lambda_{irr}}$ (Eq.9), the actinometric measurements are concentration dependent
708 whereby theoretically the slope $\beta_{\lambda_{irr}}$ will decrease with increasing concentration of the
709 actinometric species (if we assume that the remaining experimental condition are otherwise
710 similar), in agreement with the aforementioned discussion on self-photostabilising effects of
711 NIF increasing initial concentration. This observation can in fact qualitatively explain the
712 variation of the slope of the calibration curve of quinine obtained for various light energies of
713 an irradiation chamber (Azevedo Filho et al., 2011). Indeed, the authors recorded slopes of
714 0.0045 and 0.0041 Wh/m^2 for 2 % and 5% quinine solutions, respectively. This confirms their
715 conclusions about the possible consequence on ICH guidelines with respect to quinine
716 actinometry but this specific set of data does not necessarily indicate a drawback of this

717 actinometer. Consequently, our approach based on the $\beta_{\lambda_{irr}}$ factors shows the need for a
718 recalibration of the quinine actinometer or the development of more adequate actinometers (as
719 stipulated by ICH guidelines (ICH, 1996) as it reads: *alternative validated chemical*
720 *actinometers (to quinine) can be used*). Such new systems should take into account four
721 important factors, namely (i) the photochemical mechanism and/or species present in the
722 reactive medium, (ii) the concentration of the actinometric species in solution, (iii) the
723 wavelength variability of the actinometer's quantum yield and absorptivity, (iv) the number of
724 absorbing species in the medium, and (v) the optical path length (l_{irr}) of the actinometric cell
725 (i.e. the shape, volume and material of the cell should be considered and standardised).

726

727 Finally, the usefulness of Eq.7 has been investigated in relation to photostability measurements.
728 It is known that one way of protecting NIF from light is achieved by introducing in the drug's
729 formulation an amount of photoprotective excipients such as dyes (Piechocki and Thoma,
730 2010; Tonnesen, 2004; Albini and Fasani, 1998; Thoma and Klimek, 1991; Rowe et al., 2003).
731 The available literature reports on the effect of excipient-dyes and food colouring materials on
732 improving NIF photostability have been conducted using either large wavelength-span
733 irradiation lamps or filters. Besides, the data reported therein were estimations based on
734 thermal zero- and first-order reaction models, usually taking into account only the fraction of
735 the kinetic data corresponding to the early reaction stages. In one study, a method based on a
736 Stern-Volmer function type was proposed for this kind of evaluations under the assumption
737 that the quenching of NIF photoreaction by the dye was a diffusion controlled process
738 (Mielcarek et al., 2005). Up to date there are no standardised methods (ICH, 1996) to evaluate
739 and rationalise the effect of competitors (excipients) for light absorption responsible for

improving the photostability of drugs in general and those obeying AB(1Φ) kinetics in particular.

In the present study we aimed also at establishing a reliable way to quantify and rationalise such effects.

Photostabilization can be viewed as a reduction of the photodegradation reaction's rate-constant ($k_{Drug}^{\lambda_{irr}}$). Accordingly, Eqs. 6 and 8 should inform about the factors that affect such reduction. This can be achieved by reducing the values of the following quantities:

(i) the quantum yield ($\Phi_{Drug\rightarrow PP}^{\lambda_{irr}}$), which means that the molecule absorbs the light but the gained energy does not lead to photoreaction. For instance, this can be achieved by either quenching the excited-state or hampering any structural changes that might be required in the course of the phototransformation of the mother compound into the product.

(ii) the absorption coefficient ($\varepsilon_{Drug}^{\lambda_{irr}}$), which can be affected by some medium effects but these are not usually expected to be dramatic. Therefore, significant changes in $\varepsilon_{Drug}^{\lambda_{irr}}$ can only be achieved by chemically modifying the drug. Such a process, however, will raise questions on the potency of the drug and might have unwanted consequences on the biological activity of the new compound. Otherwise, the reduction of $\varepsilon_{Drug}^{\lambda_{irr}}$ can be achieved by either modifying the light source (its wavelength range) to avoid the absorption spectrum of the drug or completely removing the light (as expected to happen with an opaque packaging).

762 (iii) the optical path length ($l_{\lambda_{irr}}$), is naturally reduced in solid-state materials and non-stirred
763 solutions, since the first layers of the material exposed to light are responsible for the
764 absorption of most of the available irradiation light. This effect should be more pronounced for
765 highly concentrated formulations and/or those with a smaller exposure surface. However, such
766 a reduction in the overall reaction-rate in the bulk of the material can still yield a significant
767 amount of photoproducts in the first exposed layers; which might still raise concerns on the
768 toxicity of the generated photoproduct levels.
769
770 (iv) the radiant power ($P_{\lambda_{irr}}$), which can be reduced by three ways (iv-a) opaque packaging,
771 (iv-b) reduction of the light intensity either by reducing the power of the incident light or
772 changing its wavelength range (e.g. red light), and by (iv-c) competitive absorption by
773 excipients and chemicals in the formulation or in the immediate packaging material. For the
774 latter cases, the absorption spectra of drug and light-absorbing competitors should overlay. In
775 addition, the competitor molecule should best be chemically, photochemically and biologically
776 inert. If they happen to have photoproducts, the latter should be biologically safe.
777
778 (v) the photokinetic factor ($F_{\lambda_{irr}}$), which depends on the total absorption ($A_{tot}^{\lambda_{irr}/\lambda_{irr}}$) of all
779 absorbing species in the formulation. As $A_{tot}^{\lambda_{irr}/\lambda_{irr}}$ increases, the value of $F_{\lambda_{irr}}$ decreases and
780 therefore, an increase in the initial concentration of the drug should lead to a slow down of the
781 photoreaction (as discussed above).
782
783 It is also evident that photostability is not necessarily achieved by the effect of a single factor
784 amongst the set mentioned above but it can be improved by an optimised combination of the
785 concomitant/additive effects due to several factors.

The conclusions, reached here for unimolecular reactions, can most likely be generalised to any photoreaction, irrespective of the mechanism and the number of photoproduced species. This hypothesis can be supported by considering the rate-law models obtained for isosbestic irradiation conditions (since the integrated rate laws for non-isosbestic irradiations are not yet available). Indeed, in such conditions, exponential models are generally obtained. Their characteristic rate-constants are expressed in similar mathematical formulations to those derived for Eqs. 6 and 8. A good example can be found for reactions involving three (ABC) photoactive species linked by six reversible photo- and thermal reaction steps, the so called ABC(6Φ,6Δ) system, and any of its sub-mechanisms (Maafi and Brown, 2005).

Solutions of NIF in the presence of various concentrations of TRZ, SSY or QY were irradiated at 390 nm, a wavelength where only NIF absorbs (Fig. 5). Since in our experiment only the trace of NIF is observed (not the absorbance of the dye, taken as part of the blank experiment, which incidentally shows an advantage over separation techniques), we propose that the treatment of such NIF kinetic data is performed using Eq.7 where its rate-constant equation has been modified in order to take into account the presence of the dye in solution (Eq.10).

$$k_{NIF}^{\lambda_{irr}} = \Phi_{NIF\rightarrow PP}^{\lambda_{irr}} \times \varepsilon_{NIF}^{\lambda_{irr}} \times l_{\lambda_{irr}} \times P_{\lambda_{irr}} \times F_{\lambda_{irr}}^{dye} \qquad (Eq.10)$$

where $F_{\lambda_{irr}}^{dye}$ is calculated using Eq.2 with the constant $A_{Dye}^{\lambda_{irr}/\lambda_{irr}}$ replacing the original $A_{tot}^{\lambda_{irr}/\lambda_{irr}}$.

In order to rationalise the application of our approach, the effect of dye concentration (which is constant for a given experiment) has been evaluated by testing Eqs. 7 and 10 on RK synthetic traces that describe the reactive system irradiated at wavelengths where the initial drug species and the dye absorb. The generated RK data have been well fitted by the model equations. Also, a good linear relationship can be found between $k_{NIF}^{\lambda_{irr}}(j)$ and $F_{\lambda_{irr}}^{dye}(j)$, generally for dye absorbances below *c.a* 2.5 ($F_{\lambda_{irr}}^{dye} > 0.4$), which represents the limit of applicability of Eqs.7 and 10 with regards to the value of $F_{\lambda_{irr}}^{dye}$.

This means that Eqs. 7 and 10 can be reliably applied within the dynamic ranges of organic dyes (since, generally, linearity ranges of calibration graphs for organic molecules, including TRZ, SSY and QY, do not reach the 2.5 limit in absorbance of the compounds).

The model (Eqs.7 and 10) fitted well the experimental traces of NIF in the presence of various amounts of dyes (Table 4, Fig.5). This confirms that the model equation (Eq.7) is suitable to describe this kind of kinetics obtained in the presence of a photo- and thermally- stable excipient.

This conclusion is confirmed by the linear correlation, obtained for the different dye concentrations, for the rate-constant values determined from the fitting of the experimental traces (390/390) with model Eq.7, against the corresponding photokinetic factors ($F_{\lambda_{irr}}^{dye}$) calculated with the dyes absorbances at the irradiation wavelength (Fig.10). These linear

graphs, characterised by intercepts close to zero and correlation coefficients close to unity, indicate the reliability of the proposed model (Eqs.7 and 10).

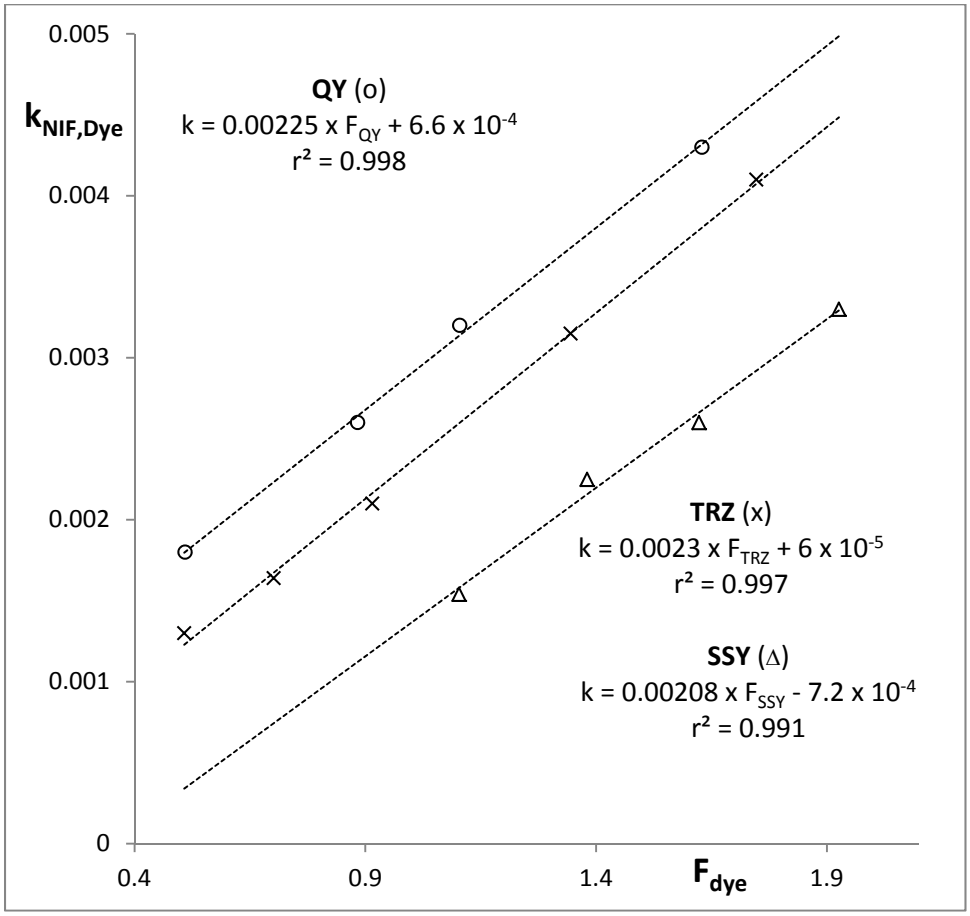

Figure 10: Linear relationships between the photokinetic factor of QY, TRZ and SSY measured at various dye concentrations ($1.14x10^{-5}$ – $1.24x10^{-4}$ M) against the overall kinetic rate-constant of NIF transformation in presence of the dye. Data taken from Table 4. λ_{irr} / λ_{obs} = 390/390.

Only small variations between the slope values (< 10%) were observed for our series of dyes and up to 80 % reduction of NIF reaction rate-constant values were achieved (Table 4). There is, however, some variation on the intercepts of the lines (Fig. 10). The intercepts can be used to estimate the values of NIF rate-constants in the presence of an infinite concentration of the

842 dyes. If this is theoretically possible, it remains a hypothetical estimation because the useful
843 dyes' concentrations for this type of studies should be limited to their respective linearity
844 ranges, as indicated above.

845

846 Our findings on the effect of TRZ, SSY and QY concentrations mean also that these dyes
847 represent good candidates to protect NIF from photolability for irradiation in the spectral
848 region 360 – 400 nm (where the self-photostabilising effect of NIF's increasing concentration
849 is not effective).

850

851 It is therefore clear that the most important factor in these experiments seem to be the value of
852 the absorbance of the dye at the irradiation wavelength (via the variation of the value of $F_{\lambda_{irr}}^{Dye}$)
853 rather than the dyes' chemical nature (TRZ and SSY are sodium salts whereas QY is neutral).
854 In addition, these results strongly suggest that the photochemical mechanism of NIF is not
855 affected by the presence of the dyes used in this study (i.e. NIF converts via a unimolecular
856 mechanism).

857

858 Therefore, the present approach may set a reliable tool to evaluate and quantify the effect of a
859 given stable excipient on the photostatbility of a drug obeying a unimolecular
860 phototransformation.

861

862 The method based on a Stern-Volmer type function proposed for a similar purpose (Mielcarek
863 et al., 2005), does not allow a direct measurement of the reaction rate-constant. In fact, the
864 assumption made here about the dynamic quenching of NIF photoreaction by the dye is

865 somewhat unnecessary since in principle the drug can be protected by the dye species that
866 filters the light available for absorption by NIF even if this dye species is used as a physical
867 light-filter outside the formulation (i.e. not necessarily in the solution/formulation of the drug,
868 it may be placed in the plastic material protecting the tablet (Tonnesen, 2001). These
869 observations may introduce some doubts on the reliability of the quantifications of the
870 photoreaction slowdown using an approach based on a Stern-Volmer type function.
871
872
873

5. CONCLUSION

The kinetic rate-law model (Eq.7) proposed in this study completes an already existing set of equations to study kinetic traces of unimolecular photoreactions AB(1Φ) subjected to isosbestic and non-isosbestic irradiation for cases where only one or both species absorb. The new semi-empirical model (Eq.7) has been intensively and successfully tested with synthetic RK data for validation.

The spectrokinetic method was successfully shown to be able to deliver a number of reactions attributes without the need for prior separation of the reactive species.

The analysis of models and data lead to the proposal of a new Φ-order kinetics specific to unimolecular photoreactions of the AB(1Φ) type

The new model was found very useful to describe the photokinetic behaviour of NIF. It has allowed the reliable determination of the values of some essential photoreactions parameters including photochemical quantum yields.

The conversion of NIF has been proven to obey a unimolecular mechanism based on the treatment of the kinetic data. The investigation of NIF has revealed that the drug is mainly photochemically active when irradiated in the spectral region situated in the UVA-visible (280 – 400 nm). The determined quantum yields of photoconversion ranged from 0.004 – 0.1

in the UVB-UVC and 0.3 – 0.5 in the UVA-visible regions. The variation of NIF quantum yields with wavelength was modelled by a sigmoid equation that predicts NIF quantum yield at any wavelength where the drug absorbs.

The effect of excipients on the reduction of the rate-constant of NIF has been established to depend on the absorbance of the excipient at the irradiation wavelengths. These results may suggest that it would be possible to virtually stop the photoreaction of NIF if a highly absorbing species in the UVA-visible range is used.

This study has also provided evidence for reaction self-rate reduction. This has been found to be due to the direct effect of the drug concentration on the photokinetic factor. The higher the drug's concentration the lower the value of $F_{\lambda_{\mathrm{irr}}}^{\mathrm{PP}}$ (Eq.7) and therefore the lower the reaction overall rate-constant, $k_{\mathrm{NIF}}^{\lambda_{\mathrm{irr}}}$ (Eq.8).

Finally, NIF has shown good potential to be used as an actinometer for low radiant power values (ranging between 5 x10^{-8} and 9 x 10^{-7} einstein s^{-1} dm^{-3}) for the 280 – 400 nm wavelength range. The actinometric approach developed here for NIF can easily be extended to other drugs obeying a similar type of photochemical processes. It hopefully opens a way for developing new drug-actinometers.

915 **REFERENCES**

916

917 Albini A., Fasani E., 1998. Drugs Photochemistry and Photostability. The Royal Society of
918 Chemistry, Cambridge.

919 Azevedo Filho CA., De Filgueiras Gomes D., De Melo Guedes J.P., Batista R.M.F., Santos
920 B.S., 2011. Considerations on the quinine actinometry calibration method used in
921 photostability testing of pharmaceuticals. J. Pharm. Biomed. Ana. 54, 886-888.

922 Baertschi SW., 1997. Commentary on the quinine actinometry system described in the ICH
923 draft guidelines on photostability testing of new drug substances and products. Drug
924 Safety. 1, 193-195.

925 Baertschi SW, Alsante KM, Tonnesen HH., 2010. A critical assessment of the ICH guidelines
926 on photostability testing of new drug substances and products (Q1B) : recommendation for
927 revision. J. Pharm. Sci. 99, 2934-2940.

928 De Vries H., Van Henegouwen G.M.J.B., 1998. Photoactivity of nifedipine in vitro and in vivo.
929 J. Photochem. Photobiol. B: Biol. 43, 217-221.

930 Dhuna M., Beezer A.E., Connor J.A., Clapham D., Courtice C., Frost J., Gaisford S., 2008.
931 LED-array photocalorimetry: Instrument design and application to photostability of
932 Nifedipine. J. Pharm. Biomed. Ana. 48, 1316-1320.

933 Fasani E., Dondi D., Ricci A., Albini A., 2006. Photochemistry of 4-(2-nitrophenyl)-1,4-
934 dihydropyridines. Evidence for electron transfer and formation of an intermediate.
935 Photochem. Photobiol. 82,225-230.

936 Fasani E., Albini A., Mella M., 2008. Photochemistry of Hantzsch 1,4-dihydropyridines and
937 pyridines. Tetrahedron. 64, 3190-3196.

938 Glass B.D., Novak Cs., Brown M.E., 2004. The thermal and photostability of solid
939 pharmaceuticals – A review. J. Therm. Anal. Cal. 77, 1-24.

940 Gorner H., 2010. Nitro group photoreduction of 4-(2-nitrophenyl)- and 4-(3-nitrophenyl)-1,4-
941 dihydropyridines. Chem. Phys. 373, 153-158.
942 ICH, 1996. Guidelines for industry: Q1B photostability testing of new substances and products.
943 Fed. Regist. 62, 27115-27122.
944 Kawabe K., Nakamura H., Hino E., Suzuki S., 2008. Photochemical stabilities of some
945 difydropyridine calcium-channel blockers in powdered pharmaceutical tablets.J. Pharm.
946 Biomed. Anal. 47, 618-624.
947 Krufurst A., Kuhan J., 1983. Quantum chemical interpretation of electronic absorption spectra
948 of the hantzsch dihydropyridines. Coll. Czech. Chem. Commun. 43, 1422-1428.
949 Kuhn H.J., Braslavsky S.E., Schmidt R., 2004. Chemical actinometry. Pure and appl. Chem.
950 76, 2105-2146.
951 Maafi M., 2008. Useful spectrokinetic methods for the investigation of photochromic and
952 thermo-photochromic spiropyrans. Molecules. 13, 2260-2302.
953 Maafi M., 2010. The potential of AB(1Φ) systems for direct actinometry. Diarylethenes as
954 successful actimometers for the visible range. Phys. Chem. Chem. Phys. 12, 13248–13254.
955 Maafi M, Brown RG., 2005. General analytical solutions for the kinetics of AB(k,Φ) and
956 ABC(k,Φ) systems. Int. J. Chem. Kinet. 37(3), 162-174.
957 Maafi M., Brown RG., 2007. The kinetic model for AB(1Φ) systems. A Closed-form
958 integration of the differential equation with a variable photokinetic factor. J. Photochem.
959 Photobiol. A: Chem. 187, 319-324.
960 Maafi M, Brown RG., 2008. Kinetic analysis and kinetic elucidation options for AB(1k,2Φ)
961 systems. New Spectrokinetic methods for photochromes. Photochem. Photobiol. Sci. 7,
962 1360 – 1372.

963 Majeed I.A., Murray W.J., Newton D.W., Othman S., Al-Turk W.A., 1987.
964 Spectrophotometric study of the photodecomposition kinetics of nifedipine. J. Pharm.
965 Pharmacol. 39, 1044-1046.
966 Matsuda Y., Teraoka R., Sugimoto I., 1989. Comparative evaluation of photostability of solid-
967 state nifedipine under ordinary and intensive light irradiation conditions. Int. J. Pharm. 54,
968 211-221.
969 Mattos C.B., Deponti V.B., Barreto F., Simoes C.M.O., Andrighetti-Frohner C.R., Nunes R.J.,
970 Steindel M., Teixeira H.F., Koester L.S., 2012. Development of a stability-indicating LC
971 method for the determination of a synthetic chalcone derivative in a nanoemulsion dosage
972 form and identification of the main photodegradation product by LC-MS. J. Pharm. Biom.
973 Anal., 70, 652-656.
974 Mauser H., Gauglitz G., 1998. in Comprehensive Chemical Kinetics, Vol. 36, Photokinetics:
975 Theoretical Fundamentals and Applications, Ed. R.G. Compton and G. Hancock.
976 Amesterdam-New York-Oxford-Shannon-Singapore-Tokyo: Elsevier.
977 Mielcarek J., Augustyniak W., Grobelny P., Nowacka G., 2005. Photoprotection of 1,4-
978 dihydropyridine derivatives by dyes. Int. J. Pharm. 304, 145-151.
979 Onoue S., Igarashi N., Yamauchi Y., Murase N., Zhou Y., Kojima T., Yamada S., Tsuda Y.,
980 2008. In vitro phototoxicity of dihydropyridine derivatives: a photochemical and
981 photobiological study. Eur. J. Pharm. Sci. 33, 262-270.
982 Piechocki J.T., Thoma K., 2010. Pharmaceutical Photostability and Photostabilisation
983 Technology. Informa Healthcare, London.
984 Pietta P., Rava A., Biondi P., 1981. High-performence liquid chromatography of nifedipine, its
985 metabolites and photochemical degradation products. J. Chrom. 210, 516-521.
986 Pizarro-Urzua N.A., Nunez-Vergara L.J., 2005. Nifedipine and nitrodipine reactivity towards
987 singlet oxygen. J. Photochem. Photobiol. A: Chem. 175, 129-137.

988 Rowe R.C., Sheskey P.J., Weller P.J., 2003. Handbook of pharmaceutical excipients (third
989 Ed.): Pharmaceutical Press and American Pharmaceutical Association.

990 Sangoi M.S., Todeschini V., Goelzer G.K., Steppe M., 2013. Photochemistry of a novel
991 antimuscarrinic drug fesoterodine and identification of its photodegradation products by
992 LC-ESI-MS studies. J. Photochem. Photobiol. A: Chem., 256, 16-22.

993 Shamsipur M., Hemmateenejad B., Akhond M., Javidnia K., Miri R., 2003. A study of the
994 photodegradation kinetics of nifedipine by multivariate curve resolution analysis, J. Pharm.
995 Biom. Anal. 31, 1013-1019.

996 Souza M.J.E., Souza P.S., Adams A.I.H., Bergold A.M., 2010. Photodegradation kinetics of
997 sodium ceftiofur in aqueous solution determined by LC method. The Open Antimicrobial
998 Agents Journal. 2, 1-7.

999 Teraoka R., Matsuda Y., Sugimoto I., 1988. quantitative design for photostabilization of
1000 nifedipine by using titanium dioxide and/or tartrazine as colourants in model film coating
1001 systems. J. Pharm. Pharmacol. 41, 293-297.

1002 Thatcher S.R., Mansfield R.K., Miller R.B., Davies C.W., Baertschi SW., 2001.
1003 Pharmaceutical photostability: a technical guide and practical interpretation of the ICH
1004 guidelines and its application to pharmaceutical stability. Pharm. Technol. 25, 98-110.

1005 Thoma K., Klimek R., 1991. Photostabilization of drugs in dosage forms without protection
1006 from packaging. Int. J. Pharm. 67, 169-175.

1007 Tonnesen H.H., 2001. Formulation and stability testing of photolabile drugs. Int. J. Pharm.
1008 225, 1–14.

1009 Tonnesen H.H., 2004. Photostability of Drugs and Drug Formulations (second Ed.). CRC
1010 Press, London.